ORIGINAL PAPER: SOL-GEL AND HYBRID MATERIALS FOR OPTICAL, PHOTONIC AND OPTOELECTRONIC APPLICATIONS

Inorganic-organic hybrid polymers for printing of optical components: from digital light processing to inkjet 3D-printing

Matthias Klein[1] · Sönke Steenhusen[1] · Peer Löbmann [1]

Abstract

Solvent-free inorganic-organic hybrid polymers were prepared for digital light processing (DLP) and ink-jet printing. The resins were characterized in terms of viscosity, surface tension, and refractive index. Optical bulk components were prepared with both printing techniques and compared regarding their surface roughness and optical scattering. The haze of DLP-samples can be avoided by inkjet 3D printing. Moreover, different quantum dots (QD) could be incorporated into resins; DLP resulted in complex 3D assemblies.

Graphical Abstract

Solvent-free inorganic-organic hybrid polymers were prepared for digital light processing (DLP) and ink-jet printing. Optical bulk components were prepared with both printing techniques. Different quantum dots (QD) could be incorporated into resins; DLP resulted in complex 3D assemblies.

Highlights

- Synthesis of solvent-free inorganic-organic hybrid resins.
- Viscosity and surface tension suitable for DLP and ink-jet technology.
- Quantum dots can be incorporated to result in functional composites.
- Printing of bulk optical components.

✉ Peer Löbmann
    peer.loebmann@isc.fraunhofer.de

[1] Fraunhofer Institut für Silicatforschung Neunerplatz 2, 97082 Würzburg, Germany

1 Introduction

For the preparation of optical components, transparent organic polymers such as polycarbonate (PC), Zeonex® (COP—Cyclo Olefin Polymer) and poly(methyl methacrylate) often are processed by molding or injection molding [1]. These processes, however, suffer from a low geometrical flexibility and may require time-consuming

post-processing steps such as polishing or deburring. Therefore, flexible additive manufacturing processes are advantageous that allow the custom manufacturing of optical elements. For example digital light processing (DLP) has extensively been applied to prepare Poly(meth) acrylate components [2–5].

However, these polymers have some disadvantages, such as high shrinkage [6] and yellowing under strong light intensity [7, 8]. In addition, their refractive index can only be tuned in a narrow range and their thermal stability is low. In all these respects, inorganic-organic hybrid polymers can offer significantly better properties: Due to their partially inorganic constituents their mechanical strength exceeds most purely organic polymers so that they are commonly applied as scratch-resistant coatings [9–11]. Due to their thermal stability and resistance to yellowing they may further be used as matrix material for LED phosphors in lighting technology [12]. By introducing transition metal oxides the refractive indices can raised by about 0.2 [13].

Up to now, transparent hybrid polymers have mainly been used as thin films for optical applications: Significant amounts of solvent that originate from hydrolysis and condensation reactions strongly hinder the defect-free consolidation to dense bulk materials. It is possible to remove volatile components from inorganic-organic hybrid polymer formulations. The resulting resins, though, normally exhibit a high viscosity that prevents the application of the aforementioned printing technologies [14].

In this paper, we describe the so far first sol-gel synthesis of two closely related hybrid polymer resins, that are solvent-free, nevertheless have low viscosities and can be processed by DLP and ink-jet printing.

2 Experimental procedure

2.1 Resin synthesis

2.1.1 Chemicals

3-(dimethoxy(methyl)silyl)propyl methacrylate (ALFA, 98% purity), CdSe/ZnS alloyed, hydrophobic quantum dots (QD) (Plasmachem, >99% purity), Dimethoxymethylsilan (ABCR, 99% purity), methoxytrimethylsilane (Sigma-Aldrich, 97% purity), hydrochloric acid 0.5 mol/l (Roth, >99% purity), ethyl acetate (Merck, >99,5% purity), TPO-L (BASF, purity n.a.) were used as purchased. 3-methacryloyloxypropyltrimethoxysilane (Momentive Performance Materials, purity n.a.) and Dimethoxydiphenylsilan (ABCR, 97% purity) were distilled before use.

2.1.2 Synthesis of DLP resin

First, 49.68 g (0.20 mol) of 3-(dimethoxy(methyl)silyl)propyl methacrylate together with 48.87 g (0.20 mol) of dimethoxydiphenylsilane were placed in a three-neck flask and 5.76 g of 0.5 mol/L hydrochloric acid, corresponding to 0.32 mol H_2O, was added. The mixture was then stirred for 10 min until a clear solution was obtained. Then, the mixture was heated in a 90 °C oil bath for 24 h. To stop the reaction, 240 ml of ethyl acetate was added and the mixture was transferred to a separatory funnel. The solution was then washed by adding 100 ml of water and shaking to remove the acid. This step was repeated a total of five times until a neutral pH was achieved. The remaining water was then separated as far as possible with the aid of a hydrophobic filter. The crude product was then distilled in several steps on the rotary evaporator. First, 130 mbar and 70 °C were set for 2 h. Then the vacuum was reduced to 40 mbar for 1 h. Finally, to evaporate the remaining water a high vacuum of 5–6×10^{-2} mbar was created using an oil pump and held for 1.5 h. At the end, the resin could be filtered through a 0.2 μm filter at 5 bar nitrogen and 1 wt.% TPO-L was added.

2.1.3 Synthesis of ink-jet resin

The second synthesis was analogous but with the following reactands: 27 mol% 3-(dimethoxy(methyl)silyl)propyl methacrylate, 13 mol% Dimethoxydiphenylsilan, 47 mol% Methoxytrimethylsilan, 13 mol% Dimethoxymethylsilan, 0.5 eq (with regard to Si-O groups) 0.5 mol/l HCl.

2.1.4 Quantum dot-composites

9 mg of the commercially purchased QD from Plasmachem were placed into a round bottom or pear shaped flask and dissolved with a few drops of THF. Then, 3 g of the resin was added. The dispersion was then treated in an ultrasonic bath for 15 min, after which the solvent was removed at the rotary evaporator at 45 mbar and 70 °C oil bath temperature. Finally, the composite was again treated in the ultrasonic bath for 15 min and 1 wt.% TPO-L was added. The mixtures showed no sedimentation and could be processed without any additional steps after several months of storing.

2.2 Sample preparation

2.2.1 3D printing

The DLP-3D-printing was performed on Rapidshape 3D Rapid Prototyping & Manufacturing System S60-LED. The layer height was 20 μm and the exposure time was 10 s per layer.

Table 1 Properties of DLP and ink-jet resin

	Viscosity at 20 °C [mPas]	Surface tension at 20 °C [mN/m]	Refractive index at 589 nm	Density at 20 °C [kg/m^3]	Transmittance at 589 nm (1 mm thickness) [%]	Ohnesorge number (21 µm nozzle size)
DLP resin	278	26.0	1.503	1068	92.0	11.33
Ink-jet resin	37	24.2	1.471	1013	92.4	1.63

2.2.2 Inkjet

Inkjet experiments were performed on the Dimatix DMP 2831 printer. The cartridges used are piezo-driven with 16 10-picoliter nozzles spaced at 254 µm. The waveforms used to drive the piezo crystals of the cartridges varied according to the printing ink. The applied voltage was also adjusted to the samples and was 15–25 V. The y-spacing of the individual nozzles was between 20 and 50 µm. Prints were made on PET film or borofloat glass.

2.2.3 Ink-jet 3D-printing

The ink-jet resin was printed with a Pixdro LP50 Inkjet Printer using a Konica Minolta KM512 LH printing head. The material was printed layer by layer which were cured for 4 s with a 395 nm LED. The substrate temperature was 30 °C.

2.2.4 Doctor blading

For transmittance measurements resins were casted into a mold of 1 mm thickness and the exceeding resin was removed with a doctor blade. The mold was covered with a ETFE-foil and cured for 2 min in a Fe-vapor-lamp-oven.

2.3 Material characterization

2.3.1 Laser scanning microscope (LSM)

LSM images were acquired on the Keyence 3D laser scanning microscope VK-X100K/X200K. Objectives with magnification levels of 10×, 20×, 50×, and 150× were used to capture various levels of detail. The measurements could be processed and evaluated via the instrument-specific software VK-Analyzer.

2.3.2 Transmittance and Haze

UV/Vis spectra or the transmission of the corresponding samples were measured on the UV-3100 instrument from SHIMADZU. The layers or moldings were clamped in the beam path of the instrument and measured in the spectral range between 300 and 800 nm.
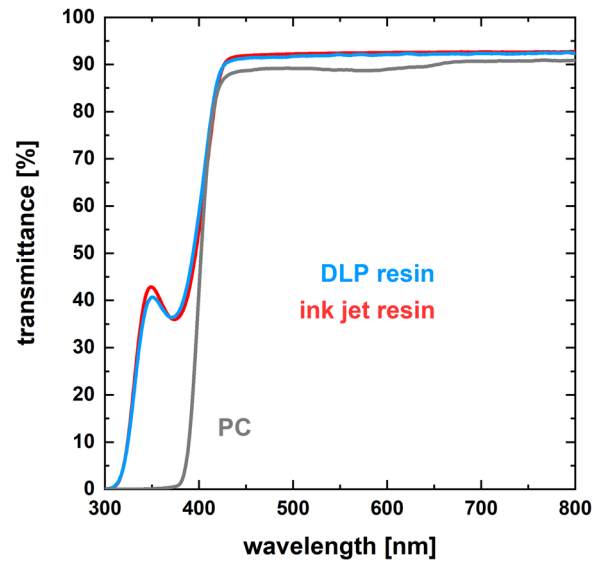

Fig. 1 Transmittance of molded bodies (thickness 1 mm) prepared from DLP- and ink-jet resins in comparison to polycarbonate (PC)
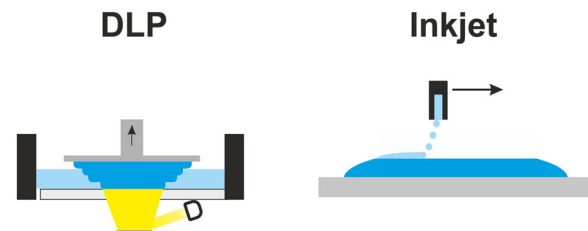

Fig. 2 Schematic representation of DLP processing (left) and ink-jet printing (right)

2.3.3 Viscosity

Viscosity measurements were carried out on the Bohlin CVO 10. For this purpose, the liquid resin was applied to the cone-plate system with 4°/40 mm inclination/diameter. For the measurements at 20 °C, shear stresses of 5–100 Pa were then set constant according to the viscosity of the samples and tenfold determinations were made.

2.3.4 Refractive index

Refractive indices were determined on the ATAGO Abbe refractometer DR-A1-Plus. The liquid samples were applied

to the prism and measured at three different wavelengths, 486 nm, 589 nm, and 656 nm.

2.3.5 Surface tension

The surface tensions were measured with a Dynometer from Byk, catalogue number 1910, with a transducer number 1922. The ring method from Lecomte De Noüy [15] was used.
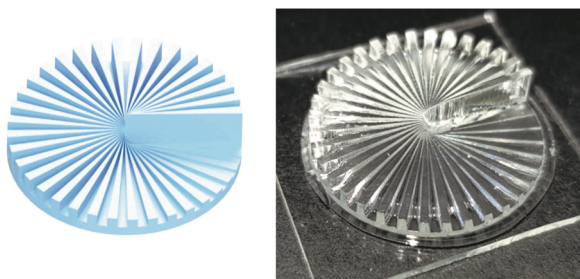

Fig. 3 CAD image of a Siemens star structure (*left*) and photograph of the respective DLP print with a diameter of 1.5 cm (*right*)
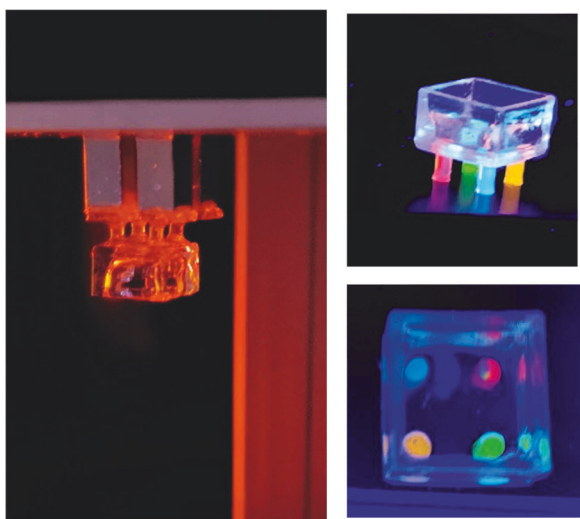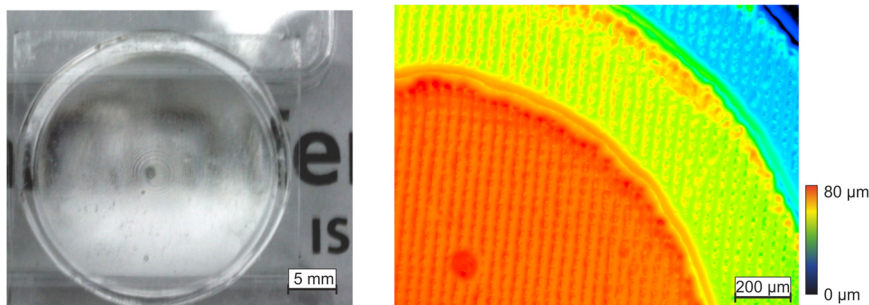

Fig. 4 Prototype of a sensor array as lifted from the DLP device (*left*) and detail images of the component showing luminescence properties (*right*). The edge length of the container is 10 mm

3 Results and discussion

The two resins under investigation are quite similar and originate from empirical experimental series in which it was tried to reduce the viscosity of the DLP resin. Therefore, the chain length was limited by introducing methoxytrimethylsilane precursors. Also, the inorganic network was reduced by using only precursors with two Si-O-groups. In addition, dimethoxydimethylsilane was introduced for its low monomeric friction coefficient. The properties of both materials are summarized in Table 1. Their viscosities are far below other solvent-free inorganic-organic hybrid polymer resins reported in the literature [16].

Free-standing bulk samples of 1 mm thickness were prepared by casting over an area of 100×100 mm². They did not crack throughout UV-curing and subsequent manual handling, their respective transmittance are shown in Fig. 1. At wavelengths above 450 nm for both bulk samples a transparency above 90% is realized, i.e., a raw transmission of >98% if Fresnel reflections are taken into account.

In the left part of Fig. 2 the schematic representation of DLP processing is shown. A build plate, which serves as substrate, is immersed into a resin bath. Through the transparent resin vat bottom polymerization is induced by a digital mirror device (DMD) arranged UV light source. The three-dimensional structure of the work piece is created by local UV exposure in conjunction with the vertical withdrawal of the specimen holder from the vat. The maximum structural accuracy is thus given by the resolution of the DMD and the possible layer thickness.

To prove the feasibility of DLP printing of complex geometries, a Siemens star type structure was chosen. The particular CAD design is given along with the outcome of the printing experiment in Fig. 3. It can be seen that the complicated microstructure is reproduced with high accuracy.

For biomedical applications, sensors incorporating QD, which fluoresce in different wavelengths, combined with a spectrometer or light intensity measuring device can be used to build for example a biomedical sensor. By using resins doped with different nanoparticles DLP offers the possibility to prepare laterally microstructured 'lab on a chip' sensors (Fig. 4). The component contains different foot

Fig. 5 Photograph of a lens (radius 12.5 mm) prepared by DLP print (*left*) and LSM image of the lens surface (*right*)

structures with QDs emitting at 480, 530, 580, and 630 nm, the edge length of the container is 10 mm.

For optical elements such as lenses, smooth surfaces are important to prevent scattering phenomena. In Fig. 5 the photograph of a convex lens prepared by DLP is shown alongside with an LSM (laser scanning microscopy) image of the surface at higher magnification. Because the curvature is realized by the successive hardening of layers with different lateral sizes, the formation of steps is inevitable. The LSM image indicates a step height of 20 µm witch correlates to the printing layer thickness. This causes some surface roughness resulting in the scattering of light. In addition, you can see a

pattern of small squares on the height image on the right side which is caused by the single mirrors of the DMD.

These problems could be reduced by the merging of adjacent droplets and the smoothing by surface tension during ink-jet printing. In the right part of Fig. 2 a schematic representation of this process is given. As the UV-curing is performed after the printing process of each layer, the ink has time for relaxation, hence self-smoothening of the surface.

The resin used for the DLP process, however, is too viscous and no drops can be formed with the printer nozzle. For this reason, the synthesis was modified resulting in a formulation of lower viscosity of 37 mPas (Table 1). This results in an Ohnesorge number [17] of 163 compared to 1133 of the DLP-resin which can be lowered below 1.00 by heating up the nozzles to get the resin jetable. In Fig. 6 the droplet formation of the ink-jet resin during the printing process is shown. It could be observed, that a droplet with a tail is forming within 20 ms. The tail generates a satellite droplet beginning at about 50 s.

A lens from the inkjet material with 10 mm radius was then printed via inkjet processing. An image and LSM-image is shown in Fig. 7. Here no visual steps but a smooth surface can be seen compared to the DLP-printed lens.

Fig. 6 Droplet formation of ink-jet resin during printing process

Fig. 7 Photograph of a lens (radius 10.0 mm) prepared by ink-jetprinting (left) and LSM surface image (right)
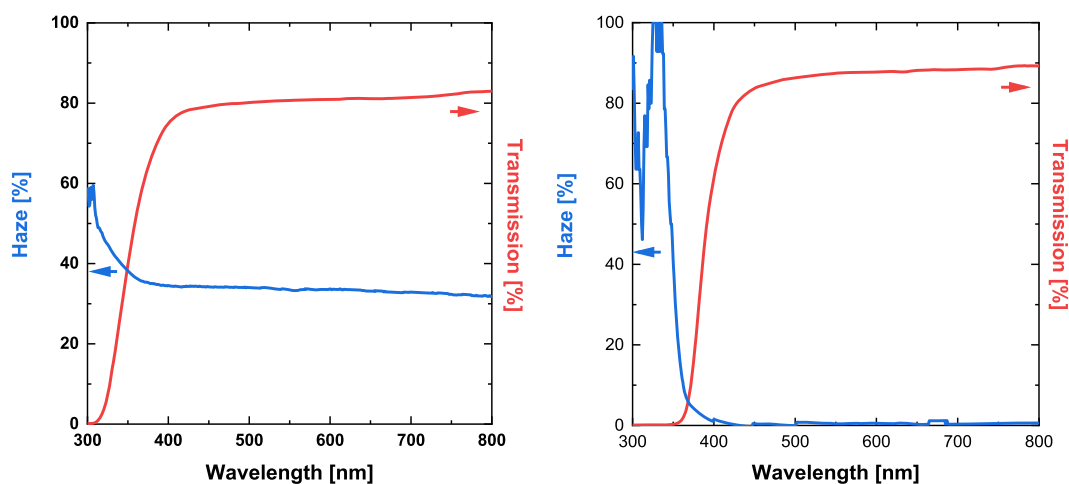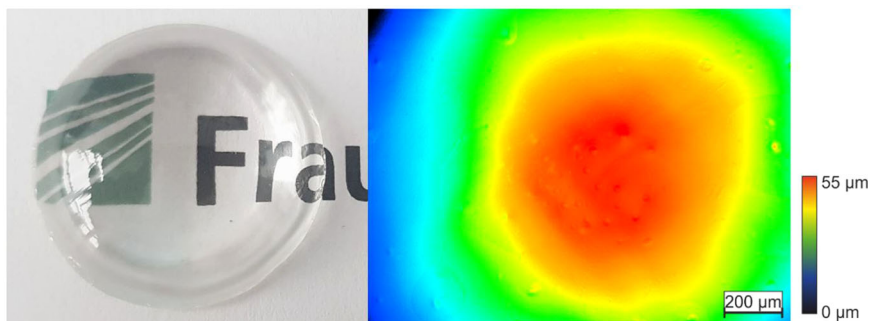

Fig. 8 Haze and transmission of a lens prepared by DLP (left) processing in comparison to a specimen obtained by ink-jet printing (right)

The transmission and haze of these two lenses are compared in Fig. 8. Surface roughness caused by the layer steps produces surface scattering. This results in a higher haze value of the lenses. Accordingly it is shown that the steps from the DLP process (Fig. 5) lead to a high haze value of >30% compared to the nearly 0% haze value of the lens manufactured by inkjet printing (Fig. 8). The lower transmission of the lens compared to the flat molded bodies is caused by the light refraction of the lens.

4 Conclusions

The so far first sol-gel synthesis of two closely related solvent-free hybrid polymer resins suitable for the fabrication of optical components in DLP and inkjet processes is reported. For this purpose, a resin with a viscosity of 213 mPas was synthesized as a basis, which is suitable for DLP printing. This brings the disadvantage of process-related step formation in the production of curved surfaces, which increases the haze and thus decreases the transmission. For these reasons, the resin was optimized for inkjet application, whereby the surfaces can be created significantly smoother and thus the transmission increases. In addition, fluorescent QD could be incorporated into the material, opening up new areas of application, such as the production of biomedical sensors on a chip.

Compliance with ethical standards

Conflict of interest The authors declare no competing interests.

Publisher's note Springer Nature remains neutral with regard to jurisdictional claims in published maps and institutional affiliations.

References

1. Uusimäki J, (2019) 3D-printing of plastic optical components & comparison to traditional manufacturing methods
2. Gibson I, Rosen D, Stucker B (2015) Additive Manufacturing Technologies, Springer New York, New York, NY
3. Ligon SC, Liska R, Stampfl J, Gurr M, Mülhaupt R (2017) Polymers for 3D printing and customized additive manufacturing. Chemical reviews 117:10212–10290
4. Melchels FPW, Feijen J, Grijpma DW (2010) Biomaterials. 31, 6121
5. Pandey R (2014) Photopolymers in 3D printing applications
6. Schmidt C, Scherzer T (2015) Influence of age on resection of colorectal liver metastases. J Polym Sci Part B: Polym Phys 53:729–739
7. Heinrich A, Rank M, Maillard P, Suckow A, Bauckhage Y, Rößler P, Lang J, Shariff F, Pekrul S (2016) Advanced Optical Technologies.5
8. Koleske JV (2002) Radiation Curing of Coatings. ASTM International, Bridgeport, NJ
9. Schmidt H (1994) Multifunctional inorganic-organic composite sol-gel coatings for glass surfaces. J Non-Crystalline Solids 178:302–312
10. Haas K-H, Amberg-Schwab S, Rose K, Schottner G (1999) Surface and Coatings Technology. 72
11. Haas K-H, Wolter H (1999) Current Opinion in Solid State and Materials Science. 571
12. Kräuter G, Eberhardt A, Peskoller F, Güldal NS, Lell A, Ritasalo R, Pilvi T, Römer M, Domann G, Löbmann P (2021) Sol–gel matrix for YAG:Ce phosphors in pc-LEDs. J Sol-Gel Sci Technol 97:458–465
13. Lee S, Shin H-J, Yoon S-M, Yi DK, Choi J-Y, Paik U (2008) Refractive index engineering of transparent ZrO_2–polydimethylsiloxane nanocomposites. J Mater Chem 18:1751
14. Hoath SD (2016) Fundamentals of Inkjet Printing
15. Lecomte du Noüy P (1925) J General Physiol. 625
16. Han X, Wang L, Liu Y, Zhang H, Wang J, Jian X, Zhao M (2008)
17. Ohnesorge WV (1936) Die Bildung von Tropfen an Düsen und die Auflösung flüssiger Strahlen. Z angew Math Mech 16:355–358